

Precision loss measurements in short lengths of optical fibre by reflectometry without using Rayleigh scattering

B.G. Gorshkov, G.B. Gorshkov, K.M. Zhukov

Abstract. To improve accuracy of light attenuation measurements in optical fibres, especially in short ones, tens and hundreds of metres in length, we propose rejecting a conventional reflectometric approach based on Rayleigh scattering intensity measurements. To this end, we propose for the first time the use of boson peaks in Raman scattering, which, on the one hand, produce no interference effects and no related noise in reflectograms, and, on the other, lie within the C-band. Even at a fibre length as short as 50 m, the attenuation measurement error does not exceed 0.002 dB km^{-1} . We demonstrate the possibility of compensating for the temperature variation of boson peak intensity by concurrently obtaining a reflectogram for the anti-Stokes line of the fundamental Raman band.

Keywords: optical fibre, optical reflectometry, Raman scattering.

1. Introduction

The possibility of obtaining reflectograms via Rayleigh scattering intensity measurements was first demonstrated by Personick [1]. Since then, time-domain reflectometers intended for evaluating transmission losses in optical fibre have become very customary in building optical communication links. Their characteristics are usually quite consistent with practical needs. There is however the problem of measuring the attenuation of light per unit length of optical fibre in short segments (tens to hundreds of metres) with sufficient accuracy (down to hundredths of a decibel per kilometre), and it is of great current interest. The accuracy of optical loss measurements in single-mode fibre with reflectometers based on Rayleigh back-scattering recording is limited for two main reasons. One of them is residual polarisation sensitivity of the real reflectometer design. This reason can be eliminated via depolarisation (due to both averaging over the spectrum and time averaging–scrambling). The other reason has a more fundamental character. As shown earlier [2, 3], the use of Rayleigh scattering always results in noiselike reflectograms, and the level of such ‘noise’, which cannot be eliminated by signal accumulation, is higher at a smaller width of the light source spectrum. The emission

spectrum cannot be extended by more than tens of nanometres without leaving the range of interest (usually, the C-band: 1525–1565 nm). Moreover, this is ineffective. Another approach is to degrade spatial resolution, e.g. by increasing the probe pulse duration, but it is unacceptable in the case of short lengths of fibre. Thus, the problem in hand cannot be resolved using Rayleigh scattering.

As shown earlier [2], far less noisy reflectograms can in principle be obtained by measuring the power of Stokes or anti-Stokes Raman scattering lines. Since scattering is due to interaction of light with optical phonons, which have a random phase after each scattering event, there are no ‘frozen-in’ back-scatter coefficient fluctuations [2] provided averaging is done over many implementations. However, both lines in question lie beyond the C-band, which may be unacceptable.

It is known that, in addition to Raman scattering, light is scattered in optical media by acoustic phonons (Brillouin scattering). Reflectograms can, in principle, be obtained at frequencies of this scattering, which differ only slightly from Rayleigh frequencies (10–11 GHz for the C-band in silica glass fibre). Unfortunately, the use of Brillouin scattering requires expensive components and complex signal processing procedures (see e.g. Budylin et al. [4]) and is thus hardly suitable for solving the problem in hand.

In this paper, we propose for the first time obtaining reflectograms at frequencies of boson peaks in Raman scattering. A spontaneous Raman spectrum of silica glass fibre, with focus on boson peaks, was obtained by Gorshkov et al. [5]. In those experiments, an argon laser ($\lambda = 510 \text{ nm}$) was used. Figure 1 presents the Raman spectrum of silica glass

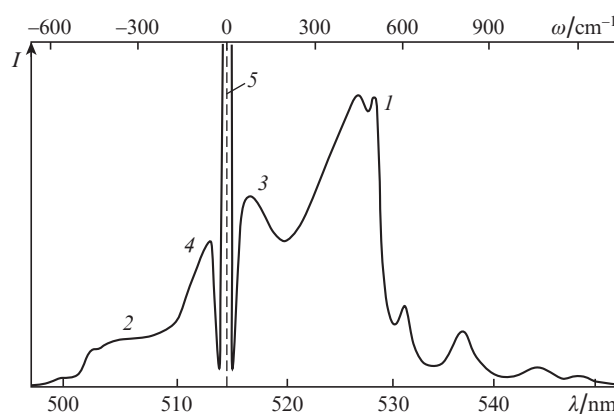


Figure 1. Spontaneous Raman spectrum of silica glass fibre: (1, 2) Stokes and anti-Stokes Raman signals, (3, 4) Stokes and anti-Stokes peaks, (5) excitation light.

B.G. Gorshkov A.M. Prokhorov General Physics Institute, Russian Academy of Sciences, ul. Vavilova 38, 119991 Moscow, Russia; e-mail: gorgb@petrofibre.ru;

G.B. Gorshkov PetroFibre Ltd, Klinskii proezd 7, 301664 Novomoskovsk, Tula region, Russia;

K.M. Zhukov Laboratory of Electronic and Optical Systems Ltd, Spartakovskaya pl. 14/4, 105082, Moscow, Russia

Received 10 October 2018; revision received 6 November 2018

Kvantovaya Elektronika 49 (6) 581–584 (2019)

Translated by O.M. Tsarev

fibre from Ref. [5]. The upper (frequency) scale is versatile and rather adequately represents characteristic Raman shifts. Figure 1 shows Stokes and anti-Stokes Raman signals [curves (1) and (2), respectively] and Stokes and anti-Stokes boson peaks [curves (3), (4)]. The origin of these peaks was analysed previously [5], together with temperature dependences of their intensity.

The frequency shift of the boson peaks is about 100 cm^{-1} , which corresponds to a wavelength shift of the order of ten nanometres in the C-band. This is important because, in the case of a probe wavelength near 1550 nm, all of the scattered light of the boson peaks falls in the C-band. Thus, both the probe signal and scattered light lie within the range under consideration.

2. Experimental

Figure 2 shows a schematic of the experimental setup for time-domain reflectometry. A distributed feedback laser diode driver (1) emitting at 1551 nm, with a bandwidth within 1 nm, generates 40-ns pulses. After an erbium-doped fibre amplifier (2), the probe light passes through a narrow-band filter (DWDM) (3) with a pass-band under 100 GHz to exclude the contribution of luminescence in the amplifier to the reflectogram (the power of the light is modulated at the pulse repetition frequency, so it can distort the reflectogram). After passing through a polarisation scrambler (General Photonics PSM-002) (4) and circulator (5), the probe light enters test fibre (6). The peak power of the probe light, 1.4 W, was limited to avoid nonlinear effects distorting reflectograms. The backscattered light passes through the circulator (5), filters (7, 8) and a switch (11) and enters a photodetector (avalanche photodiode with a transimpedance amplifier) (9). Filter 7 rejects the Rayleigh scattering signal (its pass-band is 6 nm). Filter 8, having a bonded structure, suppresses both the Stokes and anti-Stokes Raman signals, but transmits their boson peaks. The emission spectrum at the photodetector input is shown in Fig. 3. The spectrum was obtained using an ANDO AQ6319 analyser at a spectral resolution of 1 nm. The signal from the photodetector output is amplified, digitised by an analogue-to-digital converter (ADC) and fed to a computer (13).

As an example, Fig. 4 shows a reflectogram of a 1000-m length of Fujikura Future Guide LWP fibre [curve (1)]. The reflectogram was obtained via signal acquisition for 40 s using

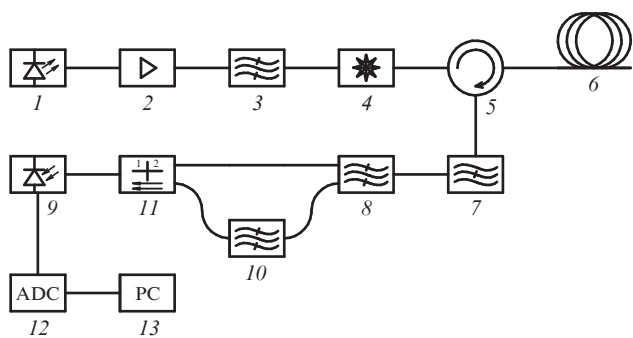


Figure 2. Schematic of the experimental setup: (1) laser diode driver; (2) erbium-doped fibre amplifier; (3) narrow-band filter; (4) polarisation scrambler; (5) circulator; (6) test fibre; (7, 8, 10) filters; (9) photodetector; (11) switch; (12) analogue-to-digital converter; (13) computer.

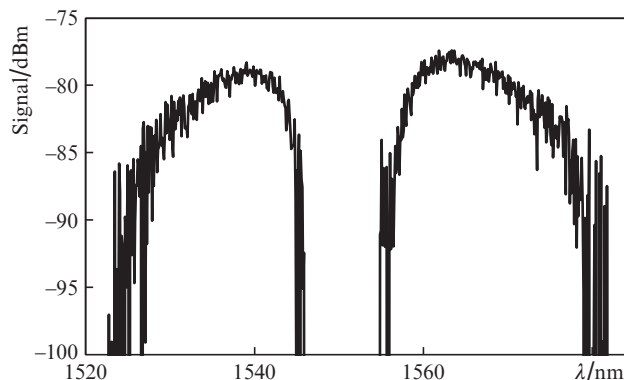


Figure 3. Backscattered Raman spectrum containing boson peaks (measured at the photodetector input).

an ADC with a clock frequency of 100 MHz. The spatial resolution of the reflectometer was estimated at 5 m. The plot has two vertical axes. The left axis represents the original signal as recorded by the ADC (with acquisition over time). The right axis corresponds to the representation utilised in conventional reflectometers, where passes of light in two directions (forward and backward) are taken into account. This axis is commonly used to represent optical losses. The reflectogram [curve (1)] has an extremely low noise level, with a root mean square (rms) deviation of 5×10^{-4} dB, or 0.01%.

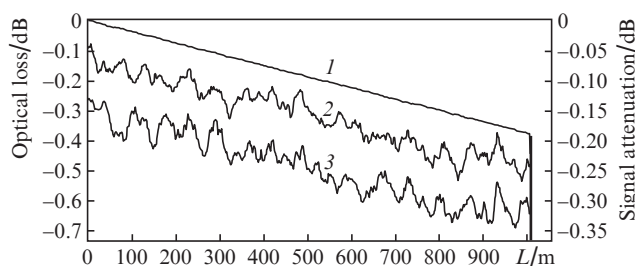


Figure 4. Reflectograms of a segment of Fujikura Future Guide LWP fibre (L is a coordinate along the fibre length). Curves (2) and (3) were obtained using a commercial reflectometer (2) with and (3) without a polarisation scrambler and are displaced downwards for clarity.

For comparison, Fig. 4 presents data obtained for the same fibre segment using a commercial reflectometer with [curve (2)] and without [curve (3)] a polarisation scrambler. The spatial resolution evaluated from an autocorrelation function is 10 m. The standard deviation of noise is 0.34% in the former case and 0.41% in the latter. The latter value is of no significant interest for us because polarisation sensitivity is determined by individual characteristics of the optical components of the reflectometer and has no fundamental limitations. Curve (2) clearly demonstrates that attenuation cannot be accurately determined at fibre lengths of tens or hundreds of metres. Note that a reflectogram obtained by connecting another (AQ7275) reflectometer, operating at the same wavelength, to the test fibre was identical to that in Fig. 4.

According to the manufacturer's data, a 25-km length of fibre (identical to the test fibre) wound onto a spool had an attenuation of 0.189 dB km^{-1} . We obtained exactly the same value by measuring attenuation in the same spool with the AQ7275 reflectometer. We take this value as a true one, from which experimental errors will be measured in what follows.

Figure 5 shows attenuation in the fibre as a function of the measurement section length. It is seen that, even at a fibre length as short as 50 m, the measurement error does not exceed 0.002 dB km^{-1} (with 0.189 dB km^{-1} taken to be the true value). Figure 6 shows the random error (standard deviation) in attenuation measurements (ten sequential measurements) as a function of fibre section length. The nonmonotonic behaviour of the curve in Fig. 6 is due to insufficient measurement statistics [cf. to curves (2) and (3) in Fig. 4].

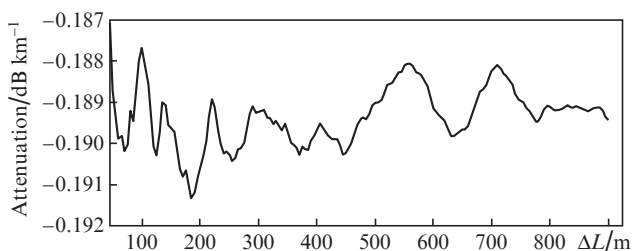


Figure 5. Measured attenuation as a function of test fibre section length L .

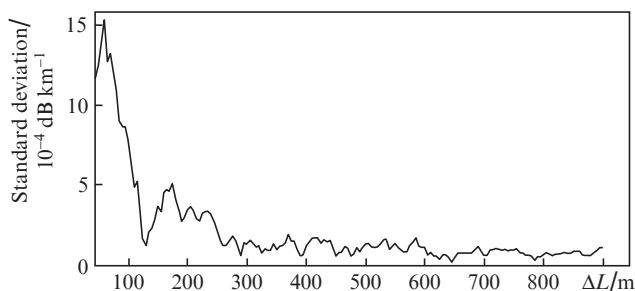


Figure 6. Standard deviation in attenuation measurements as a function of test fibre section length.

Compare now the present experimental data with a theoretical estimate of the noise level of a reflectometer utilising Rayleigh scattering. Statistical characteristics of Rayleigh scattering reflectograms for single-mode fibre can be represented by relations derived in Ref. [3], in particular by formula (19), transformed for convenience to

$$C = A\sqrt{\tau/T}, \quad (1)$$

where C is the contrast in the reflectogram, defined as the ratio of the standard deviation, σ , to the expected value of the signal, M ; τ is the coherence length of the probe light; T is the pulse duration; and A is a coefficient of order unity, weakly dependent on the shape of the spectrum and pulse shape [3]. It should be noted that relation (1) leaves out of account the impulse response of the photodetector and possible digital or analogue filtering of the signal, so, when comparison is made with experimental data, T in (1) should be taken to mean a characteristic time resolution of the instrument as a whole. Note also that the contrast described by (1) is independent of fibre characteristics (loss, numerical aperture and dopants) and is only determined by specific features of Rayleigh scattering. Given the above, calculation by formula (1) at a probe bandwidth of 10 nm yields $C = 0.32\%$, which approaches the experimentally measured 0.34%. This suggests that there is no way to reduce noise using Rayleigh scattering. Thus, our experiments demonstrate that the use of boson peaks in

Raman scattering allows the noise level to be lowered by 30 to 35 times.

It should, however, be kept in mind that, unlike in the case of Rayleigh scattering, the intensity of spontaneous scattering by phonons is temperature-dependent. In particular, the temperature coefficient of scattering intensity for boson peaks in Raman scattering is about 0.003 K^{-1} [5]. The higher the required measurement accuracy, the more stringent requirements should be placed on the temperature uniformity in the subject of the measurement. If it is a spooled fibre-optic cable, sufficient uniformity is difficult to ensure in a number of cases. One possible solution is to additionally measure the anti-Stokes Raman signal, whose spectrum is shown in Fig. 7. The spectrum was obtained using an appropriate output of filter 8 and an additional, thin-film filter (10), which cut off all wavelengths above 1500 nm. In our setup, light with the spectra shown in Figs 3 and 7 was sequentially directed to the photodetector through an optical switch (11). Since the temperature sensitivity of the intensity of the indicated anti-Stokes signal near room temperature is 0.008 K^{-1} , which considerably exceeds that for the boson peaks, there are conditions for effective compensation for temperature variations.

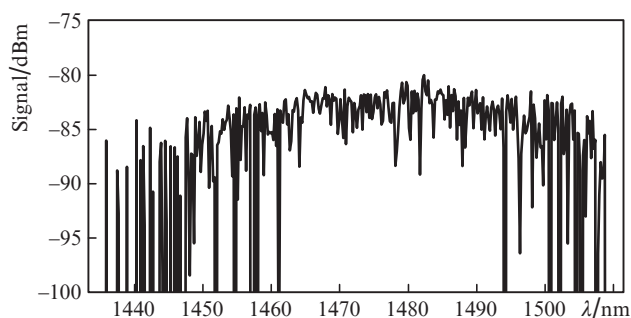


Figure 7. Spectrum of the anti-Stokes Raman signal.

To demonstrate possibilities of compensation for a nonuniform temperature profile along the fibre length, the following experiment was carried out: a 1000-m-long fibre coil was heated nonuniformly, with deviations from the average temperature of up to 3 K. It should be kept in mind that, in practice, such deviations are unacceptable. As a result, the reflectogram of the boson peaks in Raman scattering took the form shown in Fig. 8. A joint analysis of the reflectogram with one obtained for the anti-Stokes Raman signal allowed us to obtain the resultant plot for optical losses in Fig. 9, which demonstrates that temperature errors were eliminated for the most part. However, the noise level increased by six to seven times. It seems likely that refining the compensation algorithm can improve the result.

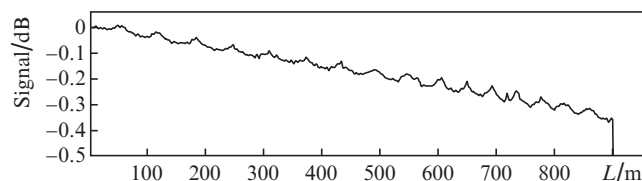


Figure 8. Original reflectogram of the boson peak in Raman scattering for a fibre segment in a nonuniform temperature field.

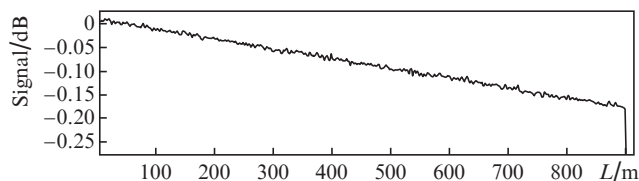


Figure 9. Reflectogram of the boson peak in Raman scattering after temperature error compensation.

Note another feature of the scheme under consideration, which makes it superior to conventional schemes based on the use of Rayleigh scattering. Since the Rayleigh scattering signal is suppressed by the filter placed before the photodetector, the reflected probe light is attenuated as well, which therefore leads to a considerable attenuation of the signal from nonuniformities, in particular from the connectors (Fresnel reflection) and low-quality fusion splices. Accordingly, there are no ‘dead zones’ after the connectors, which is important in studies of relatively short lengths of fibre. Figure 10 shows a reflectogram of two fibre segments connected by different types of FC-UPC connectors. It is seen that reflection has a very weak effect on the reflectogram. Spatial resolution can be estimated at 2 m (at a probe pulse duration of 20 ns), and there is no ‘dead zone’ after the connectors.

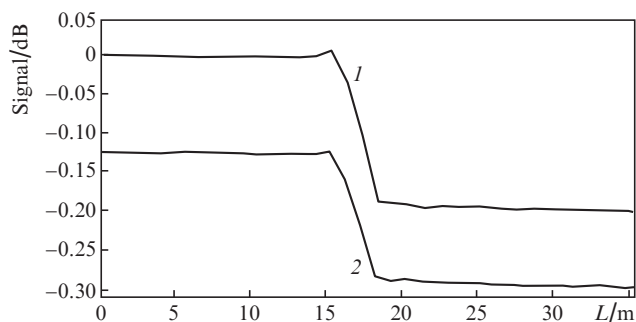


Figure 10. Reflectograms of two fibre segments connected by (1) FC-UPC connectors and (2) a UP-125/2 FC-UPC mechanical connector.

3. Conclusions

A reflectometer scheme for light attenuation measurements in optical fibre using boson peaks in Raman scattering has been proposed and studied experimentally for the first time. Eliminating interference effects related to the use of Rayleigh scattering, we have achieved high accuracy in attenuation measurements in short fibre segments, from 50 to 1000 m. A decrease in noise by more than 30 times has been demonstrated. Such measurements are performed within the C-band. A drawback to the scheme is that Raman scattering intensity is temperature-dependent. An approach has been proposed that ensures a temperature compensation for the related error by additionally obtaining a reflectogram at the wavelength of the anti-Stokes Raman signal, whose intensity is a strong function of temperature.

Acknowledgements. We are grateful to I.V. Frolov for helpful discussions.

References

1. Personick S.D. *Bell Syst. Tech. J.*, **56**, 355 (1977).
2. Busurin V.I., Gorshkov B.G., Gorshkov G.B., Grinshtein M.L., Taranov M.A. *Quantum Electron.*, **47**, 83 (2017) [*Kvantovaya Elektron.*, **47**, 83 (2017)].
3. Gorshkov B.G., Taranov M.A., Alekseev A.E. *Laser Phys.*, **27**, 085105 (2017).
4. Budylin G.S., Gorshkov B.G., Gorshkov G.B., Zhukov K.M., Paramonov V.M., Simikin D.E. *Quantum Electron.*, **47**, 597 (2017) [*Kvantovaya Elektron.*, **47**, 597 (2017)].
5. Gorshkov B.G., Gorbatov I.E., Danileiko Yu.K., Sidorin A.V. *Sov. J. Quantum Electron.*, **20**, 283 (1990) [*Kvantovaya Elektron.*, **17**, 345 (1990)].